Journal of Applied Fluid Mechanics, Vol. 8, No. 2, pp. 207-212, 2015.
Available online at www.jafmonline.net, ISSN 1735-3572, EISSN 1735-3645.
DOI: 10.18869/acadpub.jafm.67.221.20343

Effects of Radiation on Darcy-Forchheimer Convective Flow Over a Stretching Sheet in a Micropolar Fluid with Non-Uniform Heat Source/Sink

D. Pal[1†] and S. Chatterjee[2]

[1]*Department of Mathematics, Institute of Science, Visva-Bharati (A Central University), Santiniketan, West Bengal-731235, India*
[2]*Department of Mathematics, Bengal Institute of Technology and Management,* Santiniketan, West Bengal-731236, India
†*Corresponding Author Email:* dulalp123@rediffmail.com

(Received April 26, 2013; accepted July 7, 2014)

ABSTRACT

A study has been carried out to analyze the effects of viscous-Ohmic dissipation and variable thermal conductivity on steady two-dimensional hydromagnetic flow, heat and mass transfer of a micropolar fluid over a stretching sheet embedded in a non-Darcian porous medium with non-uniform heat source/sink and thermal radiation. The governing differential equations are transformed into a set of non-linear coupled ordinary differential equations which are then solved numerically. A comparison with previously published work has been carried out and the results are found to be in good agreement. The effects of various physical parameters on velocity, temperature, and concentration distributions are shown graphically.

Keywords: Porous medium; hydromagnetic; stretching sheet; micropolar fluid; convection

NOMENCLATURE

$A^\star$	coefficients of space-dependent heat source/sink
$B^\star$	coefficients of temperature-dependent heat source/sink
C_b	drag coefficient
Cp	pressure coefficient
k_1^*	vortex viscosity
N	components of microrotation
m_0	a constant
m_w	rate of mass transfer
q_r	radiative heat flux
q_w	rate of heat transfer
T	temperature of the fluid
T_w	wall temperature
j	microinertia per unit mass,
γ	spin gradient viscosity
σ	electrical conductivity of the fluid
τ_w	skin-friction on the flat plate
ρ	density of the liquid

1. INTRODUCTION

The problem of flow, heat and mass transfer of an incompressible viscous fluid on mixed convection over a stretching surface in a fluid saturated porous medium has important applications in the field of geophysics and energy related engineering problems. For instance, it occurs in the aerodynamic extrusion of polymer sheets, thermal energy storage and recoverable systems, petroleum reservoirs, continuous filament extrusion from a die, cooling of an infinite metallic plate in a cooling bath since during cooling reduction in both the thickness and width take place when these strips are sometimes stretched. The temperature distribution, thickness and width reduction are functions of draw ratio and stretching distance. In all these technologies, the quality of the final product depends on the rate of heat and mass transfer at the stretching surface. Chen and Char (1988) investigated the heat transfer on a continuous stretching surfaces with suction or blowing. More discussions and applications of convective transport in porous media can be found in the book by Nield and Bejan (1999).

Great interest has been evinced in micropolar fluids after the pioneering work by Eringen (1966) due to its occurrence in the industrial processes. This theory takes into account of local structure and microrotational effects of the fluid elements. Micropolar fluids may be used to analyze the behavior of exotic lubricants colloidal suspensions or polymeric fluid and liquid crystals. They constitute an important branch of non-Newtonian fluid dynamics in which microrotation as well as microinertia effects are exhibited. Heat and mass transfer in micropolar fluids is also important in the context of chemical engineering, aerospace engineering and also industrial manufacturing processes. A thorough review on this subject is provided by Ariman et al. (1974). Stagnation-point flow of a non-Newtonian micropolar fluid towards a stretching sheet was studied by Nazar et al. (2004).

A considerable interest has been shown in radiation interaction with convection for heat transfer in fluids. Thermal radiation on flow, heat and mass transfer processes is of major importance in the design of many advanced energy conversion systems operating at high temperature. Thermal radiation effects become important when the difference between the surface and the ambient temperature is large. Raptis (1998) considered the flow of a micropolar fluid past a continuously moving plate in the presence of radiation. Combined effects of non-uniform heat source/sink and thermal radiation on heat transfer over an unsteady stretching permeable surface was investigated by Pal (2011). It is well known that there exists non-Darcian flow phenomena besides inertia force effect and solid boundary viscous resistance. Mohammadein and Ei-Amin (2000) analyzed the problem of thermal dispersion-radiation effects on non-Darcy natural convection in a fluid saturated porous medium. The influence of thermal radiation on hydromagnetic Darcy-Forchheimer mixed convection flow past a stretching sheet embedded in a porous medium was investigated by Pal and Mondal (2011). Recently, Pal and Mondal (2012) analyzed hydromagnetic convective diffusion of species in Darcy–Forchheimer porous medium with non-uniform heat source/sink and variable viscosity. Very recently, Anjalidevi and Kayalvizhi (2013) studied effects of thermal radiation and heat source on nonlinear hydromagnetic flow over a stretching surface with prescribed heat and mass flux embedded in a porous medium.

The objective of the present paper is to study heat transfer by mixed convection from a vertical flat plate embedded in electrically conducting micropolar fluid saturated porous medium using Darcy-Brinkman-Forchheimer Boussinesq model in the presence of uniform magnetic field, non-uniform heat source/sink and thermal radiation. The nonlinearity of the basic equations and associated mathematical difficulties have led us to use numerical method. Thus the transformed dimensionless governing equations are solved numerically by using fifth-order Runge-Kutta-Fehlberg method (RKF45) method with shooting technique. The flow scenario stated above finds applications in polymer processing, metallurgical transport modeling, aerodynamic heating and many geophysical processes e.g. crude oil recovery. The present stretching sheet flow problem with heat transfer is quite important in polymer extrusion.

2. MATHEMATICAL FORMULATION AND GOVERNING EQUATIONS

We consider a steady two-dimensional mixed convection flow of an incompressible, electrically conducting micropolar fluid towards a surface coinciding with the plane y=0 and the flow region $y > 0$. The x-axis is taken in the direction along motion of the sheet and the y-axis is taken perpendicular to it. The flow is generated by the action of two equal and opposite forces along the x-axis and the sheet is stretched in such a way that the velocity at any instant is proportional to the distance from the origin ($x = 0$). Further, the flow field is exposed to the influence of an external transverse magnetic field of strength $\vec{B} = (0, B_0, 0)$. Frictional heating due to viscous dissipation and Ohmic heating due to application of magnetic field are considered in the present model. With these assumptions the governing equations are given by

(i) The equation of continuity

$$\frac{\partial u}{\partial x} + \frac{\partial \mathrm{v}}{\partial y} = 0, \tag{1}$$

(ii) The equation of momentum

$$u\frac{\partial u}{\partial x} + \mathrm{v}\frac{\partial u}{\partial y} = \left(\nu + \frac{k_1^*}{\rho}\right)\frac{\partial^2 u}{\partial y^2} + \frac{k_1^*}{\rho}\frac{\partial N}{\partial y} - \frac{\nu\varphi}{k}u - \frac{C_b}{\sqrt{k}}\varphi u^2$$

$$-\frac{\sigma}{\rho}B_0^2 u + g^*\beta_t(T - T_\infty) + g^*\beta_c(C - C_\infty) = 0 \tag{2}$$

(iii) The equation of angular momentum

$$\rho j\left(u\frac{\partial N}{\partial x} + \mathrm{v}\frac{\partial N}{\partial y}\right) = \gamma\frac{\partial^2 N}{\partial y^2} - k_1^*\left(2N + \frac{\partial u}{\partial y}\right), \tag{3}$$

(iv) The equation of energy

$$u\frac{\partial T}{\partial x} + \mathrm{v}\frac{\partial T}{\partial y} = \frac{1}{\rho C_p}\frac{\partial}{\partial y}\left(\kappa\frac{\partial T}{\partial y}\right) - \frac{1}{\rho C_p}\frac{\partial q_r}{\partial y} + \frac{\sigma B_0^2}{\rho C_p}u^2$$

$$+\frac{q'''}{\rho C_p} + \frac{\mu}{\rho C_p}\left(\frac{\partial u}{\partial y}\right)^2, \tag{4}$$

(v) The equation of mass diffusion

$$u\frac{\partial C}{\partial x} + \mathrm{v}\frac{\partial C}{\partial y} = D\frac{\partial^2 C}{\partial y^2}. \tag{5}$$

where u and v are the velocity components along the x and y directions, ρ is the density of the liquid, T is the temperature of the fluid, C_b is the form of drag coefficient which is independent of viscosity and other properties of the fluid but depends on the geometry of the medium, k is permeability of the porous medium, C_p is the specific heat at constant pressure, ν is the kinematic viscosity, σ is the electrical conductivity of the fluid, N is the components of microrotation or angular velocity whose rotation is in the direction of the x-y plane and j, γ and k_1^* are the microinertia per unit mass, spin gradient viscosity and vortex viscosity,

respectively. Furthermore, the spin gradient viscosity γ, which defines the relationship between the co-efficient of viscosity and micro-inertia is as follows (Kim and Kim (2007)), $\gamma=\mu(1+K/2)j$, where $K=k_1^*/\mu$ (>0) is the material parameter. Here all the material constants γ, μ, K, j are non-negative and we take $j = \nu/b$ as a reference length. The appropriate physical boundary conditions for the problem under study are given by

$$u = u_w = bx,\ v = 0,\ N = -m_0\frac{\partial u}{\partial y},$$

$$T = T_W = T_\infty + A_0\left(\frac{x}{l}\right)^2,\ C = C_W = C_\infty + A_1\left(\frac{x}{l}\right)^2 \text{ at } y = 0,$$

$$u \to 0,\ T \to T_\infty,\ N \to 0,\ C \to C_\infty \text{ as } y \to \infty \qquad (6)$$

The non-uniform heat source/sink q''' is given by

$$q''' = \frac{\kappa u_w}{x\nu}\left[A^*(T_W - T_\infty)e^{-\eta} + B^*(T - T_\infty)\right],$$

where $A^\star$ and $B^\star$ are the coefficients of space and temperature-dependent heat source/sink, respectively. The case $A^*> 0$ and $B^*> 0$ corresponds to internal heat generation while $A^*< 0$ and $B^*< 0$ corresponds to internal heat absorption, l is the characteristic length, T_w is the wall temperature and T_∞ is the temperature of the fluid far away from the sheet, C_w is the wall concentration of the solute and C_∞ is the concentration of the solute far away from the sheet and A_0, A_1 are constants. It should be remarked that m_0 is a constant such that $0 \le m_0 \le 1$.

2.1 Similarity Solutions for Momentum and Angular Momentum Equations

The governing Eqs. (2)-(5) admit a self-similar solution of the form

$$u = bxf'(\eta),\ v = -\sqrt{b\nu}\,f(\eta),\ \eta = \sqrt{\frac{b}{\nu}}y,\ N = bx\sqrt{\frac{b}{\nu}}g(\eta) \qquad (7)$$

where f is the dimensionless stream function and η is the similarity variable. Substituting these in Eq. (2), we obtain the following third -order non-linear ordinary differential equation:

$$f'^2 - f f'' = (1+K)f''' - Da^{-1}f' - \alpha f'^2 + K g' - Ha^2 f' + Gr_t\theta + Gr_c\varphi, \qquad (8)$$

where $Da^{-1} = \frac{\varphi\nu}{kb}$ is inverse Darcy number, $Ha = \sqrt{\frac{\sigma}{b\rho}}B_0$ is Hartmann number, $Gr_t = \frac{g^*\beta_t(T - T_\infty)}{b^2 l}$ is thermal Grashof number, $Gr_c = \frac{g^*\beta_c(C - C_\infty)}{b^2 l}$ is solutal Grashof number and $K = \frac{k_1^*}{\mu}$ is material parameter. Using the transformation (7), we obtain the ordinary differential equation of the form as follows:

$$fg - f g' = (1 + K/2)g'' - K(2g + f''). \qquad (9)$$

The appropriate boundary condition (6) now becomes

$$f(\eta)=0,\quad f'(\eta)=1,\quad g(\eta) = -m_0 f''(\eta) \quad at \quad \eta=0,$$
$$f'(\eta)\to 0,\quad g(\infty)\to 0,\quad as \quad \eta\to\infty. \qquad (10)$$

2.2 Similarity Solution of the Energy and Mass-Diffusion Equations

The thermal conductivity κ is assumed to vary linearly with temperature and it is of the form

$$\kappa = \kappa_\infty[1 + \varepsilon\theta(\eta)],$$

where $\theta(\eta) = (T - T_\infty)/(T_w - T_\infty)$ and $\varepsilon=(\kappa_w - \kappa_\infty)/\kappa_\infty$, which depends on the nature of the fluid and is a small parameter. In general, $\varepsilon > 0$ for air and liquids such as water, while $\varepsilon<0$ for fluids such as lubrication oils. Following Rosseland approximation (see Hsiao (2007)) the radiative heat flux q_r is modeled as, $q_r = -(4\sigma^*/3k^*)\partial T^4/\partial y$ where σ^* is the Stefan-Boltzmann constant and k^* is the mean absorption coefficient. T^4 can be expressed by using Taylor's series as $T^4 \cong -3T_\infty^4 + 4T_\infty^3 T$. Thus, we have from Eq. (4) as

$$u\frac{\partial T}{\partial x} + v\frac{\partial T}{\partial y} = \frac{1}{\rho C_p}\frac{\partial}{\partial y}\left(\left(\kappa + \frac{16T_\infty^3\sigma^*}{3k^*}\right)\frac{\partial T}{\partial y}\right) + \frac{\sigma B_0^2}{\rho C_p}u^2 + \frac{q'''}{\rho C_p} + \frac{\mu}{\rho C_p}\left(\frac{\partial u}{\partial y}\right)^2. \qquad (11)$$

The thermal boundary conditions for solving Eq. (11) depends on the type of heating process considered. Thus non-dimensional temperature θ(η) and concentration ϕ (η) are defined in PST case as

$$\theta(\eta) = \frac{T - T_\infty}{T_w - T_\infty},\qquad \phi(\eta) = \frac{C - C_\infty}{C_w - C_\infty}\ , \qquad (12)$$

where,

$$T - T_\infty = A_0\left(\frac{x}{l}\right)^2\theta(\eta) \quad \text{and} \quad T_w - T_\infty = A_0\left(\frac{x}{l}\right)^2, \qquad (13)$$

$$C - C_\infty = A_1\left(\frac{x}{l}\right)^2\varphi(\eta) \quad and \quad C_w - C_\infty = A_1\left(\frac{x}{l}\right)^2. \qquad (14)$$

Finally, we obtain the non-linear ordinary differential equation for θ(η) and ϕ (η) in the form

$$(1 + Nr + \varepsilon\theta)\theta'' + Pr\left(f\theta' - 2f'\theta\right) + \varepsilon\theta'^2 + Pr\,Ha^2 E_c f'^2 + (1 + \varepsilon\theta)\left(A^* f' + B^*\theta\right) + Pr\,E_c f''^2 = 0, \qquad (15)$$

$$\phi'' + Sc(\varphi' f - 2\phi f') = 0. \qquad (16)$$

Corresponding thermal boundary conditions for θ(η) and ϕ (η) are given by

$$\theta(\eta) = 1,\quad \phi(\eta) = 1 \quad at\ \eta=0, \qquad (17)$$
$$\theta(\eta)\to 0,\ \varphi(\eta)\to 0 \quad as \quad \eta\to\infty. \qquad (18)$$

(9)

Here the prime denotes the differentiation with respect to η and $E_c = \frac{b^2 l^2}{D_0 C_p}$ is Eckert number, $\Pr = \frac{\mu C_p}{\kappa_\infty}$ is Prandtl number, $Nr = \frac{16T_\infty^3 \sigma^*}{3k^* \kappa_\infty}$ is thermal radiation parameter and $Sc = \frac{\nu}{D}$ is Schmidt number.

2.3 Skin-friction Coefficient, Nusselt Number and Sherwood Number

The most important physical quantities for the problem are skin-friction coefficient (C_f), local Nusselt number (Nu_x) and local Sherwood number (Sh_x) which are defined by the following relations:

$$C_f = \frac{\tau_w}{\rho u_w^2 / 2},\ Nu_x = \frac{x q_w}{\kappa (T_w - T_\infty)},\ Sh = \frac{x m_w}{D(C_w - C_\infty)} \quad (19)$$

The skin-friction on the flat plate τ_w, rate of heat transfer q_w and rate of mass transfer m_w are given by

$$\tau_w = \left[\left(\mu + k_1^*\right)\frac{\partial u}{\partial y}\right]_{y=0},\ q_w = -\kappa\left[\frac{\partial T}{\partial y}\right]_{y=0},\ m_w = -D\left[\frac{\partial C}{\partial y}\right]_{y=0} \quad (19)$$

Thus we get from Eq. (18) as

$$C_f\, Re_x^{1/2} = (1+K) f''(0),\ Nu_x = -\sqrt{Re_x}\,\theta'(0), \quad (20)$$

where $Re_x = u_w x/\nu$ is the local Reynolds number.

3. Results And Discussions

In the present study our main focus is to analyze the effects of various physical parameters with the help of some important graphs. A comparative study of the present result with those of Ishak et. al (2008), Chen (1998) and Grubka and Bobba (1985) is performed and the results are presented in Table-1. It is clearly seen from this table that present results coincides very well with their results, which confirms that the numerical method used in the present work is accurate and perfect. Fig. 1 depicts the convergency history plot of $f'(0)$, $g(0)$, $\theta(0)$, $\phi(\eta)$. From this figure it is observed that there is no change in the value of $f'(\eta)$, $\theta(\eta)$, $\phi(\eta)$ when the value of η_∞ is increased. Thus it can be concluded that the numerical method adopted in this paper is very efficient as it has passed all the checks required for testing the efficiency of a numerical method. Fig. 2 shows the graph of velocity profile for various values of inverse Darcy number Da^{-1} and m_0. It is observed from this figure that velocity profile increases with increase in the value of m_0, whereas reverse effect is observed for increase in the inverse Darcy number. Physically, this is due to the fact that increase in the values of Da^{-1} leads to lower permeability of the porous media (i.e. Da^{-1} is proportional to $1/k$), which implies more resistance offered to the flow due to the presence of porous fiber and which leads to the deceleration in transport. Also in the limit $Da^{-1} \to 0$, the flow corresponds to the case of a vanishing porous medium which leads to the scenario of higher velocity profile in the momentum boundary layer.

Fig. 3 is the plot of $g(\eta)$ with η for different values of Gr_t and m_0. It is found that increase in the thermal Grashof number results in increase in the value of angular velocity $g(\eta)$ and peak is observed near the stretching boundary which ultimately decreases to zero away from the stretching boundary layer and thereby

Table 1 Comparison of local Nusselt number $\theta'(0)$ with *Pr* for *Ha*=0, *Sc*=0.0 and various values of *Pr* with Ishak et al. (2008), Chen (1998) and Grubka and Bobba (1985)

Pr	$\theta'(0)$			$\theta'(0)$
	Ishak et al. (2008)	Chen (1998)	Grubka and Bobba (1985)	Present Results
1	1.3333	1.33334	1.3333	1.333333
3	2.5097	2.50997	2.5097	2.509725
10	4.7969	4.79686	4.7969	4.796873

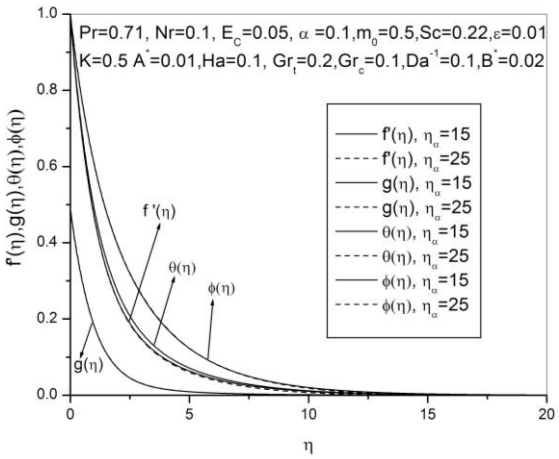

Fig. 1. Convergence history plot of $f'(\eta)$, $g(\eta)$, $\theta(\eta)$, $\phi(\eta)$ where $\eta_\alpha = \eta_\infty$.

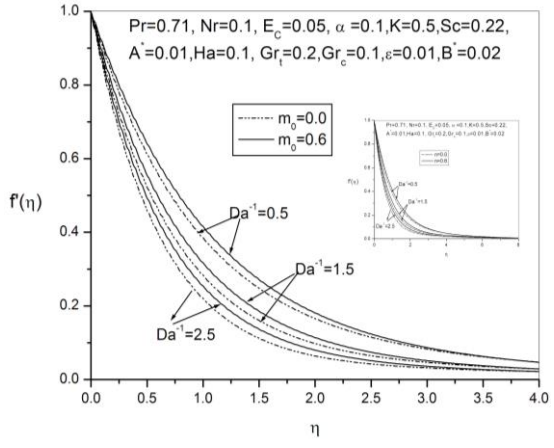

Fig. 2. Variation of f' for inverse Darcy number Da^{-1} and m_0.

matching the boundary condition as $\eta \to \infty$, for both the values of $m_0 = 0.0$ and 0.6. This shows that the thermal Grashof number boosts the microrotation values indicating that the thermal buoyancy force has an

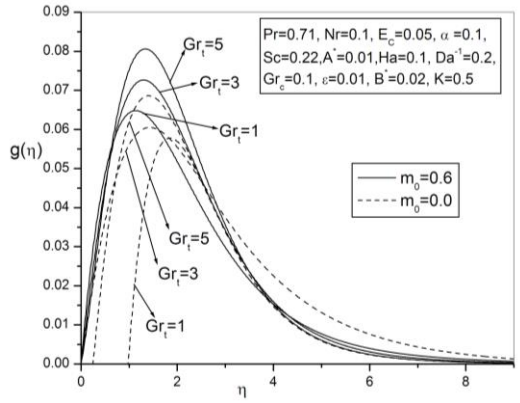

Fig. 3. Effect of $g(\eta)$ with η for different values of Gr_t and m_0 {TC "3 Effect of $g(\eta)$ with η for different values of Gr_t and n." \f f}

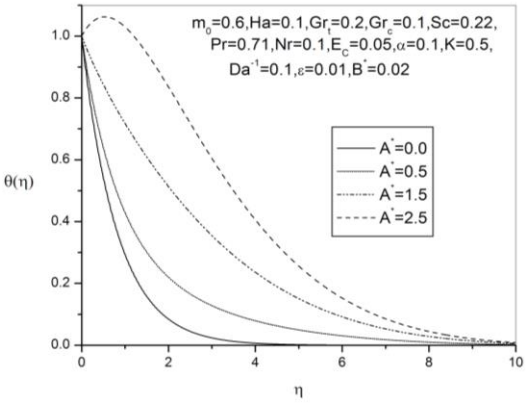

Fig. 4. Plot of temperature profiles $\theta(\eta)$ with η for various values of space-dependent non-uniform heat source parameter $A^*>=0$.

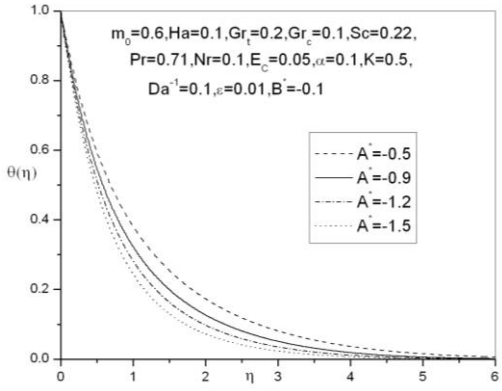

Fig. 5. Plot of temperature profiles $\theta(\eta)$ with η for various values of space-dependent non-uniform heat sink parameter $A^*<0$.

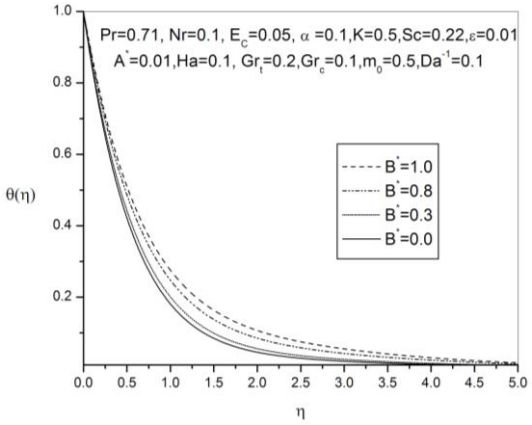

Fig. 6. Plot of temperature profiles $\theta(\eta)$ with η for various values of temperature-dependent non-uniform heat source parameter $B^*>=0$. { TC "4 Plot of temperature profiles $\Theta(\eta)$ with η for various values of A^*." \f f}

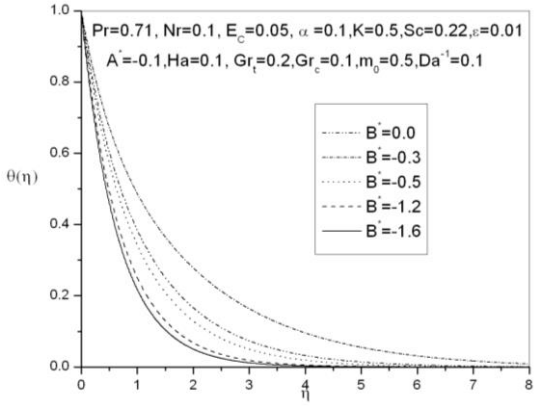

Fig. 7. Plot of temperature profiles $\theta(\eta)$ with η for various values of temperature-dependent non-uniform heat sink parameter $B^*<=0$. { TC "5 Effect of $\Theta(\eta)$ with η for different values of B^*." \f f}

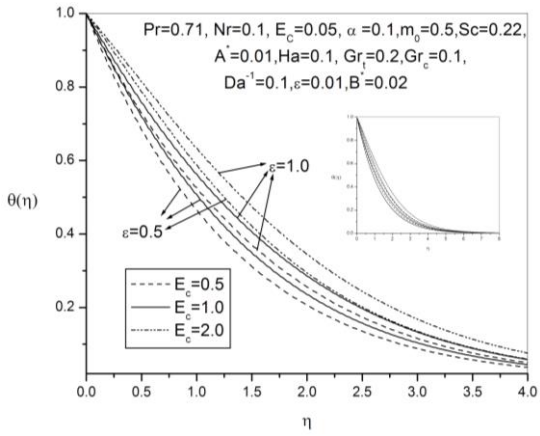

Fig. 8. Influence of porous parameter ε on temperature profile $\theta(\eta)$ with E_c.{ TC "6 Influence of porous parameter ε on temperature profile $\Theta(\eta)$ with E_c." \f f}

Fig. 8 represents the graph of temperature profile θ(η) with E_c and ε, we observe by analyzing the graph that the effect of increasing the value of Eckert number E_c is to increase the temperature distribution in the thermal boundary layer. Physical meaning is that the heat energy is stored in the fluid because of the frictional heating, so as the value of Eckert number is increased which means that there is increase in the frictional heating due to viscous dissipation thereby increases the temperature in the thermal boundary layer.

4. CONCLUSION

The present paper deals with the analysis of steady boundary layer flow, heat and mass transfer of a micropolar fluid past an impermeable stretching sheet embedded in a porous medium with magnetic field and thermal radiation effects using the Darcy-Brinkman-Forchheimer model. The governing boundary layer non-linear differential equations are solved numerically. Following conclusions are drawn from the numerical results as follows:

(i) Velocity profiles decrease with increase in inverse Darcy number Da^{-1}.

(ii) Angular velocity increases with increase in the thermal Grashof number.

(iii) Presence of space-dependent heat source parameter A^* and temperature-dependent heat source parameter B^* increase the temperature profile, whereas reverse effects are observed in the case of sink when $A^* < 0$ & $B^* < 0$.

(iv) Temperature increases with increase in the value of the Eckert number, *n* and Hartmann number.

ACKNOWLEDGEMENTS

The authors are thankful to the editor and referees for their constructive comments and suggestions, which have, lead to improvement of the paper considerably.

REFERENCES

Anjalidevi, S. P. and M. Kayalvizhi (2013). Nonlinear hydromagnetic flow with radiation and heat source over a stretching surface with prescribed heat and mass flux embedded in a porous medium. J. Applied Fluid Mechanics, 6(2), 157–165.

Ariman, T., Turk M. A. and N. D. Sylvester (1974). Application of microcontinuum fluid mechanics. Int. J. Engg. Sci., 12, 273–293.

Chen, C.H. (1998). Laminar mixed convection adjacent to vertical continuously stretching sheets. Heat Mass Trans. 33, 471-476.

Chen, C.K. and M. Char (1988). Heat transfer on a continuous stretching surfaces with suction or blowing. J. Math. Anal. Appl. 135, 568-580.

Eringen, A. C. (1966). Theory of micropolar fluids. J. Math. Mech. 16, 1–18.

Grubka, L.G. and K.M. Bobba (1985). Heat transfer characteristics of a continuous stretching surface with variable temperature. ASME J. Heat Trans. 1074, 248-250.

Hsiao, K.L. (2007) . Conjugate heat transfer of magnetic mixed convection with radiative and viscous dissipation effects for second grade viscoelastic fluid past a stretching sheet. Appl. Thermal Engg. 27, 1895–1903.

Ishak A., Nazar, R. and I. Pop (2008). Hydromagnetic flow and heat transfer adjacent to a stretching vertical sheet. Heat Mass Trans. 44, 921–927.

Kim, Y.J. and K.S. Kim (2007). Boundary layer flow of micropolar fluids past an impulsively started infinite vertical plate. Phy. Scr. 75, 132–137.

Nazar, R., Amin, N., Filip, D. and I. Pop. (2004). Stagnation-point flow of a micropolar fluid towards a stretching sheet. Int. J. Nonlin. Mech. 39, 1227–1235.

Pal, D. (2011). Combined effects of non-uniform heat source/sink and thermal radiation on heat transfer over an unsteady stretching permeable surface. Commun. Nonlinear Sci. Numer. Simul. 16, 1890-1904.

Pal, D. and H. Mondal (2011). The influence of thermal radiation on hydromagnetic Darcy-Forchheimer mixed convection flow past a stretching sheet embedded in a porous medium. Meccanica 46, 739-753.

Pal, D. and H. Mondal (2012). Hydromagnetic convective diffusion of species in Darcy–Forchheimer porous medium with non-uniform heat source/sink and variable viscosity. Intern. Commu. Heat Mass Transf. 39, 913–917.

Raptis, A. (1998). Flow of a micropolar fluid past a continuously moving plate by the presence of radiation. Int. J. Heat Mass Trans. 41, 2865–2866.

Mohammadein A. A. and M.F. El-Amin (2000). Thermal dispersion-radiation effects on non-Darcy natural convection in a fluid saturated porous medium. Trans. Porous Media 40, 153–163.

Nield, D.A. and A. Bejan, A. (1999). Convection in porous media. 2nd ed. Springer, New York.